Electronic Supplementary Material (ESI) for Dalton Transactions.

Electronic Supporting Information

Pentanuclear lanthanide pyramids based on thiacalix[4]arene ligand exhibiting slow magnetic relaxation

Jing-Yuan Ge,[a] Jing Ru,[a] Feng Gao,[a,b] You Song,[a] Xin-Hui Zhou,[c] and Jing-Lin Zuo[*a]

[a] *State Key Laboratory of Coordination Chemistry, School of Chemistry and Chemical Engineering, Collaborative Innovation Center of Advanced Microstructures, Nanjing University, Nanjing 210093, P. R. China*

[b] *School of Chemistry and Chemical Engineering, Jiangsu Normal University, Xuzhou 221116, P. R. China*

[c] *Institute of Advanced Materials, Nanjing University of Posts and Telecommunications, Nanjing 210046, P. R. China*

[*] To whom correspondence should be addressed. Email: zuojl@nju.edu.cn; Fax: +86-25-83314502.
Nanjing University.

Caption of Content

15. **Fig. S10**. Temperature-dependent in-phase χ' and out-of-phase χ'' ac susceptibility signals for **2** at the frequency of 999 Hz under zero and 1000 Oe dc field, respectively.

16. **Fig. S11**. Temperature-dependent in-phase χ' and out-of-phase χ'' ac susceptibility signals for **3** at the frequency of 999 Hz under zero and 1000 Oe dc field, respectively.

17. **Fig. S12**. Temperature-dependent in-phase χ' and out-of-phase χ'' ac susceptibility signals for **5** at the frequency of 999 Hz under zero and 1000 Oe dc field, respectively.

18. **Fig. S13**. Temperature-dependent in-phase χ' and out-of-phase χ'' ac susceptibility signals for **6** at the frequency of 999 Hz under zero and 1000 Oe dc field, respectively.

Table S1. Selected bond lengths (Å) and angles (°) for **1–3**

	1 (Dy)	**2 (Ho)**	**3 (Er)**
	Bond lengths (Å)		
Ln(1)-O(10)	2.267(7)	2.263(6)	2.276(7)
Ln(1)-O(11)	2.296(6)	2.270(6)	2.239(7)
Ln(1)-O(7)	2.326(5)	2.320(4)	2.295(5)
Ln(1)-O(6)	2.324(5)	2.320(4)	2.290(5)
Ln(1)-O(1)	2.348(5)	2.344(5)	2.344(6)
Ln(1)-O(4)	2.360(5)	2.355(5)	2.331(6)
Ln(1)-O(5)	2.508(5)	2.485(4)	2.485(6)
Ln(1)-S(1)	2.926(2)	2.9310(19)	2.911(2)
Ln(1)-Ln(2)	3.5293(8)	3.5170(7)	3.4948(8)
Ln(1)-Ln(4)	3.5386(8)	3.5204(7)	3.5085(8)
Ln(1)-Ln(5)	3.7571(8)	3.7550(7)	3.7372(8)
Ln(2)-O(13)	2.262(6)	2.253(5)	2.230(7)
Ln(2)-O(12)	2.284(6)	2.262(6)	2.265(7)
Ln(2)-O(8)	2.315(5)	2.318(5)	2.324(5)
Ln(2)-O(7)	2.333(6)	2.314(5)	2.309(6)
Ln(2)-O(2)	2.347(6)	2.336(5)	2.355(6)
Ln(2)-O(1)	2.373(5)	2.356(4)	2.327(5)
Ln(2)-O(5)	2.505(5)	2.506(4)	2.476(5)
Ln(2)-S(2)	2.964(2)	2.963(2)	2.961(2)
Ln(2)-Ln(3)	3.5384(8)	3.5186(7)	3.5049(8)
Ln(2)-Ln(5)	3.7793(8)	3.7729(7)	3.7571(8)
Ln(3)-O(15)	2.249(7)	2.259(5)	2.262(7)
Ln(3)-O(14)	2.270(6)	2.263(5)	2.251(7)
Ln(3)-O(8)	2.322(6)	2.302(5)	2.263(6)
Ln(3)-O(9)	2.324(6)	2.318(5)	2.319(6)
Ln(3)-O(3)	2.352(5)	2.357(5)	2.343(5)
Ln(3)-O(2)	2.352(5)	2.369(5)	2.341(6)
Ln(3)-O(5)	2.496(5)	2.494(4)	2.482(5)
Ln(3)-S(3)	2.939(2)	2.932(2)	2.943(3)
Ln(3)-Ln(4)	3.5438(8)	3.5340(7)	3.5090(8)
Ln(3)-Ln(5)	3.7589(9)	3.7453(8)	3.7468(9)

Ln(4)-O(16)	2.249(6)	2.250(5)	2.242(7)
Ln(4)-O(17)	2.288(7)	2.256(6)	2.271(7)
Ln(4)-O(6)	2.311(6)	2.306(5)	2.308(6)
Ln(4)-O(4)	2.318(5)	2.332(4)	2.316(5)
Ln(4)-O(9)	2.330(5)	2.321(4)	2.285(5)
Ln(4)-O(3)	2.358(6)	2.336(5)	2.333(6)
Ln(4)-O(5)	2.539(5)	2.524(4)	2.516(5)
Ln(4)-S(4)	2.950(2)	2.944(2)	2.944(2)
Ln(4)-Ln(5)	3.7692(8)	3.7666(7)	3.7503(8)
Ln(5)-O(19)	2.336(7)	2.323(6)	2.323(7)
Ln(5)-O(18)	2.332(7)	2.308(6)	2.305(7)
Ln(5)-O(20)	2.330(6)	2.313(6)	2.289(7)
Ln(5)-O(21)	2.341(6)	2.316(5)	2.282(6)
Ln(5)-O(8)	2.416(6)	2.410(5)	2.412(6)
Ln(5)-O(6)	2.430(5)	2.423(4)	2.428(5)
Ln(5)-O(9)	2.439(6)	2.426(5)	2.416(6)
Ln(5)-O(7)	2.446(5)	2.428(4)	2.406(5)
Bond angles (°)			
Ln(1)-O(1)-Ln(2)	96.76(18)	96.88(17)	96.88(19)
Ln(2)-O(2)-Ln(3)	97.7(2)	96.83(19)	96.5(2)
Ln(3)-O(3)-Ln(4)	97.6(2)	97.69(19)	97.3(2)
Ln(4)-O(4)-Ln(1)	98.30(18)	97.36(17)	98.04(18)
Ln(1)-O(5)-Ln(3)	169.4(2)	168.9(2)	168.6(2)
Ln(1)-O(5)-Ln(2)	89.51(15)	89.61(14)	89.57(18)
Ln(3)-O(5)-Ln(2)	90.07(15)	89.46(14)	89.97(17)
Ln(1)-O(5)-Ln(4)	89.03(15)	89.30(14)	89.10(18)
Ln(3)-O(5)-Ln(4)	89.47(14)	89.54(13)	89.18(17)
Ln(2)-O(5)-Ln(4)	169.6(2)	169.2(2)	168.9(2)
Ln(4)-O(6)-Ln(1)	99.6(2)	99.09(18)	99.5(2)
Ln(4)-O(6)-Ln(5)	105.3(2)	105.54(18)	104.7(2)
Ln(1)-O(6)-Ln(5)	104.4(2)	104.66(19)	104.7(2)
Ln(1)-O(7)-Ln(2)	98.50(19)	98.76(18)	98.77(19)
Ln(1)-O(7)-Ln(5)	103.9(2)	104.51(18)	105.3(2)
Ln(2)-O(7)-Ln(5)	104.5(2)	105.41(18)	105.6(2)
Ln(2)-O(8)-Ln(3)	99.5(2)	99.20(18)	99.62(19)

Ln(2)-O(8)-Ln(5)	106.0(2)	105.84(19)	105.0(2)
Ln(3)-O(8)-Ln(5)	105.0(2)	105.25(19)	106.5(2)
Ln(3)-O(9)-Ln(4)	99.18(19)	99.25(17)	99.3(2)
Ln(3)-O(9)-Ln(5)	104.2(2)	104.24(18)	104.6(2)
Ln(4)-O(9)-Ln(5)	104.4(2)	105.00(18)	105.8(2)
Ln(2)-Ln(1)-Ln(4)	90.59(2)	90.716(18)	90.39(2)
Ln(2)-Ln(1)-Ln(5)	62.395(14)	62.407(13)	62.493(15)
Ln(4)-Ln(1)-Ln(5)	62.128(16)	62.260(14)	62.248(16)
Ln(1)-Ln(2)-Ln(3)	89.64(2)	89.559(18)	89.84(2)
Ln(1)-Ln(2)-Ln(5)	61.759(15)	61.889(13)	61.916(15)
Ln(3)-Ln(2)-Ln(5)	61.713(14)	61.698(13)	62.007(15)
Ln(2)-Ln(3)-Ln(4)	90.36(2)	90.467(18)	90.21(2)
Ln(2)-Ln(3)-Ln(5)	62.297(13)	62.493(12)	62.304(14)
Ln(4)-Ln(3)-Ln(5)	62.064(13)	62.241(11)	62.144(13)
Ln(1)-Ln(4)-Ln(3)	89.41(2)	89.257(18)	89.55(2)
Ln(1)-Ln(4)-Ln(5)	61.783(14)	61.926(12)	61.868(14)
Ln(3)-Ln(4)-Ln(5)	61.770(16)	61.632(14)	62.043(16)
Ln(1)-Ln(5)-Ln(3)	83.04(2)	82.713(18)	82.67(2)
Ln(1)-Ln(5)-Ln(4)	56.089(12)	55.815(11)	55.884(13)
Ln(3)-Ln(5)-Ln(4)	56.165(15)	56.126(13)	55.814(15)
Ln(1)-Ln(5)-Ln(2)	55.847(13)	55.704(12)	55.591(13)
Ln(3)-Ln(5)-Ln(2)	55.989(16)	55.809(14)	55.689(16)
Ln(4)-Ln(5)-Ln(2)	83.44(2)	83.231(18)	82.88(2)

Table S2. Selected bond lengths (Å) and angles (°) for **4–6**

	4 (Dy)	**5 (Ho)**	**6 (Er)**
	Bond lengths (Å)		
Ln(1)-O(9)	2.184(4)	2.188(4)	2.182(4)
Ln(1)-O(6)	2.301(4)	2.289(4)	2.283(4)
Ln(1)-O(14)	2.342(4)	2.327(4)	2.314(4)
Ln(1)-O(10)	2.351(4)	2.337(4)	2.326(4)
Ln(1)-O(7)	2.359(4)	2.351(4)	2.341(4)
Ln(1)-O(13)	2.432(3)	2.406(4)	2.396(4)
Ln(1)-S(7)	2.8791(16)	2.8669(16)	2.8607(16)

Ln(1)-S(10)	2.8993(16)	2.8928(17)	2.8847(16)
Ln(1)-Ln(5)	3.5708(4)	3.5512(5)	3.5383(4)
Ln(1)-Ln(4)	3.6285(4)	3.6062(5)	3.5900(4)
Ln(1)-Ln(2)	3.6943(4)	3.6766(5)	3.6608(4)
Ln(2)-O(20)	2.289(4)	2.279(4)	2.276(4)
Ln(2)-O(19)	2.298(4)	2.293(4)	2.288(4)
Ln(2)-O(15)	2.370(4)	2.365(4)	2.351(4)
Ln(2)-O(8)	2.417(4)	2.402(4)	2.390(4)
Ln(2)-O(7)	2.421(4)	2.406(4)	2.395(4)
Ln(2)-O(21)	2.442(4)	2.427(5)	2.416(4)
Ln(2)-O(10)	2.465(4)	2.456(4)	2.448(4)
Ln(2)-O(13)	2.761(4)	2.749(4)	2.745(4)
Ln(2)-S(8)	2.9023(16)	2.8919(16)	2.8863(16)
Ln(2)-Ln(3)	3.6411(4)	3.6199(5)	3.6049(4)
Ln(2)-Ln(5)	3.7637(4)	3.7496(5)	3.7364(4)
Ln(3)-O(2)	2.190(4)	2.187(4)	2.186(4)
Ln(3)-O(8)	2.326(4)	2.309(4)	2.298(4)
Ln(3)-O(15)	2.339(4)	2.322(4)	2.322(4)
Ln(3)-O(5)	2.349(4)	2.336(4)	2.322(4)
Ln(3)-O(3)	2.362(4)	2.348(4)	2.335(4)
Ln(3)-O(13)	2.419(4)	2.413(4)	2.397(4)
Ln(3)-S(5)	2.8807(15)	2.8692(16)	2.8629(16)
Ln(3)-S(2)	2.9242(16)	2.9109(17)	2.9036(16)
Ln(3)-Ln(5)	3.5713(4)	3.5546(5)	3.5404(4)
Ln(3)-Ln(4)	3.6725(4)	3.6542(5)	3.6380(4)
Ln(4)-O(17)	2.289(4)	2.285(5)	2.279(4)
Ln(4)-O(16)	2.304(4)	2.292(5)	2.287(5)
Ln(4)-O(14)	2.383(4)	2.374(4)	2.365(4)
Ln(4)-O(6)	2.414(4)	2.403(4)	2.391(4)
Ln(4)-O(5)	2.417(4)	2.407(4)	2.397(4)
Ln(4)-O(18)	2.420(4)	2.402(5)	2.395(4)
Ln(4)-O(3)	2.477(4)	2.467(4)	2.456(4)
Ln(4)-O(13)	2.719(4)	2.706(4)	2.691(4)
Ln(4)-S(6)	2.9347(16)	2.9226(17)	2.9191(16)
Ln(4)-Ln(5)	3.7776(5)	3.7612(6)	3.7480(4)

Ln(5)-O(11)	2.187(4)	2.177(4)	2.174(4)
Ln(5)-O(4)	2.199(4)	2.187(5)	2.183(4)
Ln(5)-O(14)	2.400(4)	2.381(4)	2.375(4)
Ln(5)-O(15)	2.405(4)	2.388(4)	2.375(4)
Ln(5)-O(10)	2.567(4)	2.550(4)	2.536(4)
Ln(5)-O(3)	2.569(4)	2.546(4)	2.531(4)
Ln(5)-O(13)	2.577(4)	2.572(4)	2.563(4)
Ln(5)-S(3)	3.0129(17)	3.0070(17)	3.0045(17)
Ln(5)-S(11)	3.0446(16)	3.0341(17)	3.0290(16)
Bond angles (°)			
Ln(3)-O(3)-Ln(4)	98.70(14)	98.71(14)	98.79(14)
Ln(3)-O(3)-Ln(5)	92.70(13)	93.08(14)	93.26(14)
Ln(4)-O(3)-Ln(5)	96.92(13)	97.24(14)	97.44(13)
Ln(3)-O(5)-Ln(4)	100.80(14)	100.78(15)	100.85(15)
Ln(1)-O(6)-Ln(4)	100.58(15)	100.42(15)	100.34(15)
Ln(1)-O(7)-Ln(2)	101.22(14)	101.22(15)	101.24(15)
Ln(3)-O(8)-Ln(2)	100.27(14)	100.39(15)	100.49(15)
Ln(1)-O(10)-Ln(2)	100.15(13)	100.16(14)	100.11(14)
Ln(1)-O(10)-Ln(5)	93.00(13)	93.10(14)	93.30(13)
Ln(2)-O(10)-Ln(5)	96.79(13)	97.00(14)	97.10(13)
Ln(3)-O(13)-Ln(1)	177.87(18)	178.09(19)	177.87(18)
Ln(3)-O(13)-Ln(5)	91.19(12)	90.91(13)	91.03(12)
Ln(1)-O(13)-Ln(5)	90.88(12)	90.95(12)	90.98(12)
Ln(3)-O(13)-Ln(4)	91.05(12)	90.91(13)	91.10(12)
Ln(1)-O(13)-Ln(4)	89.38(11)	89.53(12)	89.57(12)
Ln(5)-O(13)-Ln(4)	90.95(12)	90.85(12)	90.98(12)
Ln(3)-O(13)-Ln(2)	89.07(11)	88.81(12)	88.77(12)
Ln(1)-O(13)-Ln(2)	90.47(12)	90.74(13)	90.55(12)
Ln(5)-O(13)-Ln(2)	89.60(11)	89.54(12)	89.43(11)
Ln(4)-O(13)-Ln(2)	179.43(18)	179.52(17)	179.57(18)
Ln(1)-O(14)-Ln(4)	100.32(14)	100.18(15)	100.23(14)
Ln(1)-O(14)-Ln(5)	97.70(14)	97.91(15)	97.99(14)
Ln(4)-O(14)-Ln(5)	104.33(14)	104.55(16)	104.53(15)
Ln(3)-O(15)-Ln(2)	101.30(14)	101.12(15)	100.99(15)
Ln(3)-O(15)-Ln(5)	97.68(14)	97.98(15)	97.83(14)

Ln(2)-O(15)-Ln(5)	104.04(14)	104.17(15)	104.49(15)
Ln(5)-Ln(1)-Ln(4)	63.293(9)	63.400(10)	63.437(8)
Ln(5)-Ln(1)-Ln(2)	62.376(8)	62.472(8)	62.504(8)
Ln(4)-Ln(1)-Ln(2)	96.891(9)	97.009(10)	97.126(9)
Ln(3)-Ln(2)-Ln(1)	82.780(9)	82.654(10)	82.530(8)
Ln(3)-Ln(2)-Ln(5)	57.642(8)	57.645(9)	57.632(7)
Ln(1)-Ln(2)-Ln(5)	57.203(8)	57.125(9)	57.143(8)
Ln(5)-Ln(3)-Ln(2)	62.902(8)	63.008(8)	63.049(8)
Ln(5)-Ln(3)-Ln(4)	62.847(9)	62.882(11)	62.931(8)
Ln(2)-Ln(3)-Ln(4)	97.056(9)	97.165(10)	97.270(9)
Ln(1)-Ln(4)-Ln(3)	83.257(9)	83.157(10)	83.056(9)
Ln(1)-Ln(4)-Ln(5)	57.608(8)	57.587(10)	57.610(8)
Ln(3)-Ln(4)-Ln(5)	57.266(8)	57.264(8)	57.261(7)
Ln(1)-Ln(5)-Ln(3)	85.547(8)	85.392(9)	85.218(8)
Ln(1)-Ln(5)-Ln(2)	60.420(8)	60.403(9)	60.353(8)
Ln(3)-Ln(5)-Ln(2)	59.456(8)	59.347(9)	59.320(8)

Table S3. Hydrogen-bond distances (Å) and angles (°) for **1** and **4**

Complexes	D−H···A	D−H	H···A	D···A	D−H···A
1	O22−H22···O7	0.903	2.413	3.121	135.49
	O23−H23F···Cl3	0.850	2.591	3.438	174.24
	O23−H23G···Cl8	0.850	2.117	2.958	170.10
	O24−H24C···Cl5	0.850	2.267	3.002	144.95
	O24−H24D···Cl6	0.850	2.075	2.776	139.48
	C21−H21C···Cl3	0.960	2.659	3.467	142.29
	C72−H72A···O20	0.960	2.359	3.104	133.20
	C74−H74B···O21	0.960	2.191	3.144	166.06
	C46−H46B···π	0.960	2.985	3.472	112.87
	C56−H56C···π	0.960	2.730	3.410	128.32
4	O13−H13···O6	0.816	2.306	2.736	113.46
	O14−H14P···O12	0.980	2.149	3.113	167.42
	O15−H15A···O1	0.980	2.125	3.092	168.72
	O18−H18···O25	0.820	1.760	2.578	174.64
	O21−H21···O26	0.820	1.782	2.601	177.07

O25−H25···O9	0.820	2.056	2.866	169.47
O26−H26···O2	0.820	2.006	2.826	178.82

Table S4. Shape analysis for the metal centers of **1**

ML8	SAPR-8	TDD-8	JSD-8	JBTPR-8	BTPR-8
Dy1	1.759	2.335	3.638	**1.422**	1.857
Dy2	1.875	3.051	4.234	**1.685**	2.195
Dy3	1.839	2.646	3.836	**1.551**	2.027
Dy4	1.918	2.767	4.070	**1.380**	1.944
Dy5	**0.134**	2.457	5.175	2.782	2.162

SAPR-8 (D4d): Square antiprism

TDD-8 (D2d): Triangular dodecahedron

JSD-8 (D2d): Snub diphenoid J84

JBTPR-8 (C2v): Biaugmented trigonal prism J50

BTPR-8 (C2v): Biaugmented trigonal prism

Table S5. Shape analysis for the metal centers of **4**

ML8	SAPR-8	TDD-8	JSD-8	JBTPR-8	BTPR-8
Dy1	3.988	2.172	**2.075**	2.952	2.899
Dy3	4.112	**2.057**	2.157	2.839	2.802

ML9	JCSAPR-9	CSAPR-9	JTCTPR-9	TCTPR-9	MFF-9
Dy2	**1.042**	1.088	1.825	1.690	1.649
Dy4	1.260	**1.201**	1.696	1.623	1.719
Dy5	3.070	2.665	**1.446**	3.151	3.208

JCSAPR-9 (C4v): Capped square antiprism J10

CSAPR-9 (C4v): Spherical capped square antiprism

JTCTPR-9 (D3h): Tricapped trigonal prism J51

TCTPR-9 (D3h): Spherical tricapped trigonal prism

MFF-9 (Cs): Muffin

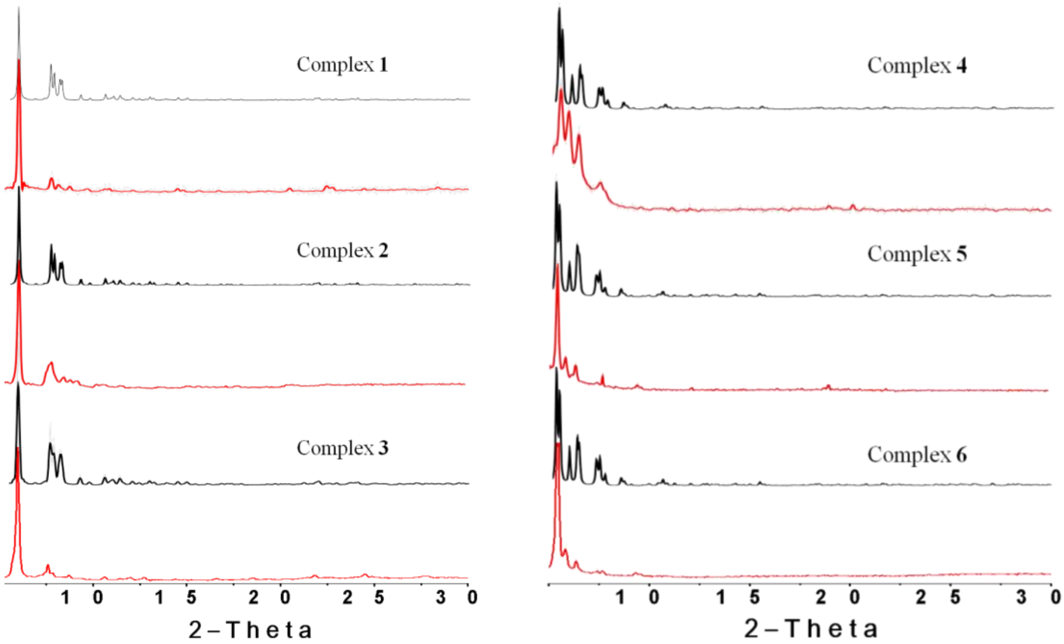

Fig. S1. The XRPD patterns (red lines) obtained from the as-synthesized solids of **1**–**6** and the simulated XRPD patterns (black lines) from single crystals of **1**–**6**.

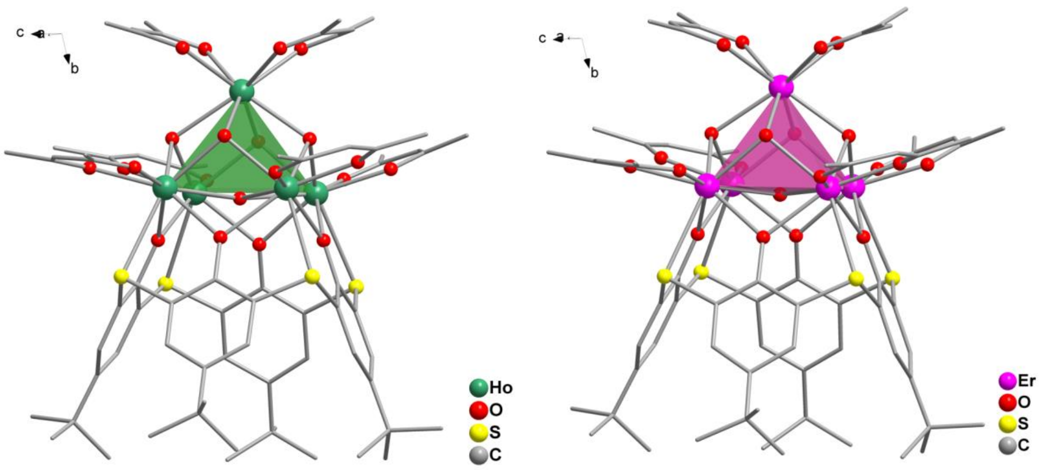

Fig. S2. The crystal structures of complexes **2** and **3**.

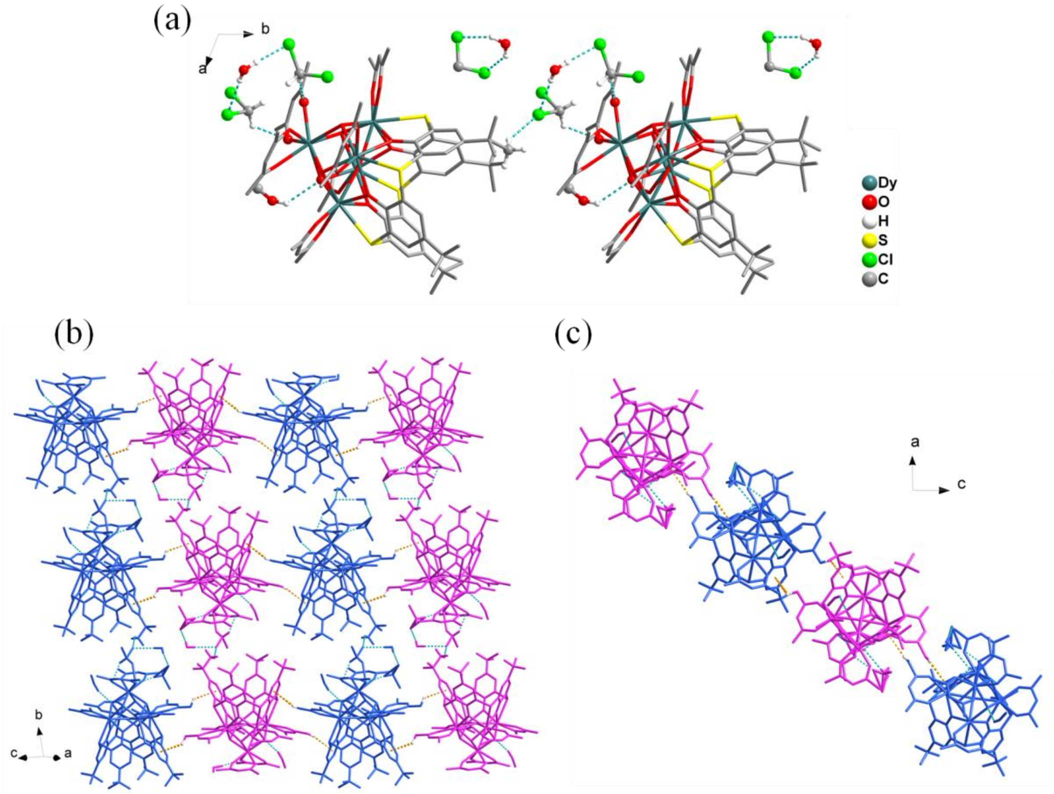

Fig. S3. (a) The neighbouring $\{Dy_5\}$ clusters are linked together through several sets of O−H···X and C−H···X (X = O and Cl) hydrogen bonds (blue dashed lines) between solvent and the framework in **1**. (b) Each $\cdots Dy_5\cdots Dy_5\cdots Dy_5\cdots$ chain stacks together *via* two sets of C−H···π interactions (orange dashed lines) in an ···ABAB··· fashion. (c) Top view of the layer.

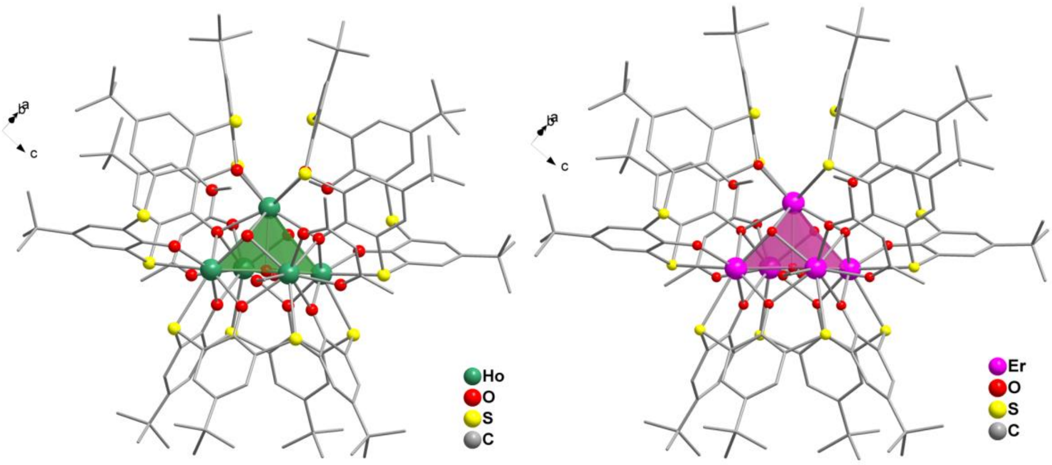

Fig. S4. The crystal structures of complexes **5** and **6**.

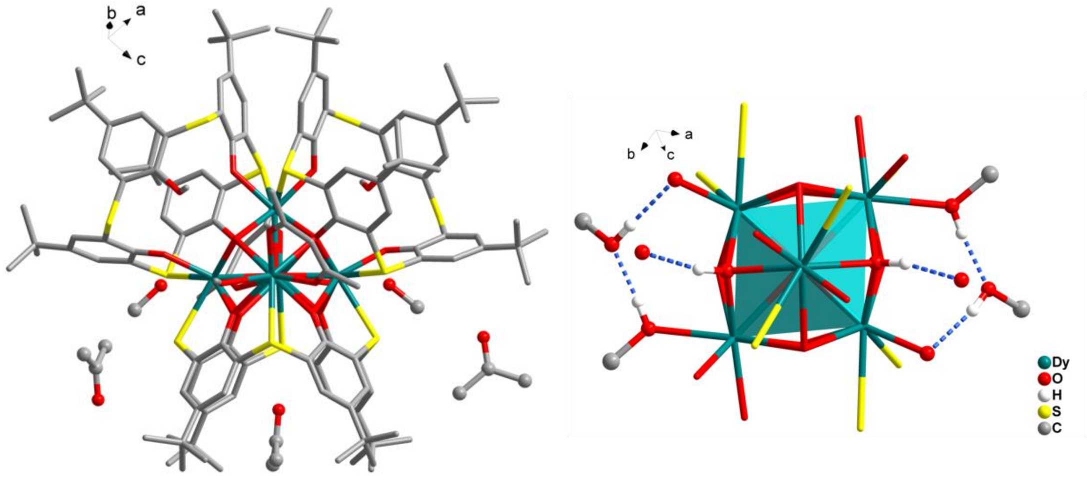

Fig. S5. In **4**, two CH_3OH and three acetone molecules exist around the $\{Dy_5\}$ cluster, and two CH_3OH molecules connect with the framework through several O−H···O hydrogen bonds (dashed lines).

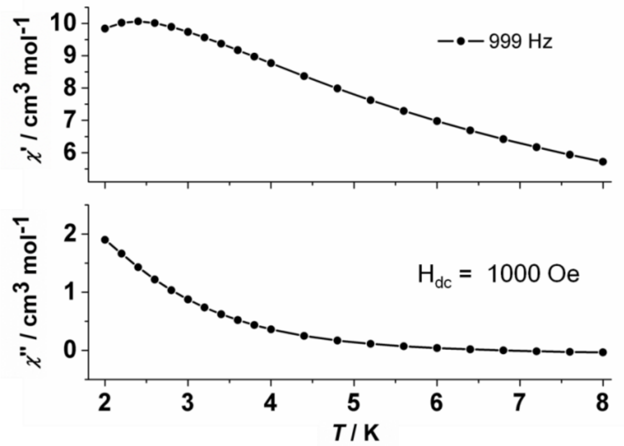

Fig. S6. Temperature-dependent in-phase χ' and out-of-phase χ'' ac susceptibility signals for **1** at the frequency of 999 Hz under 1000 Oe dc field.

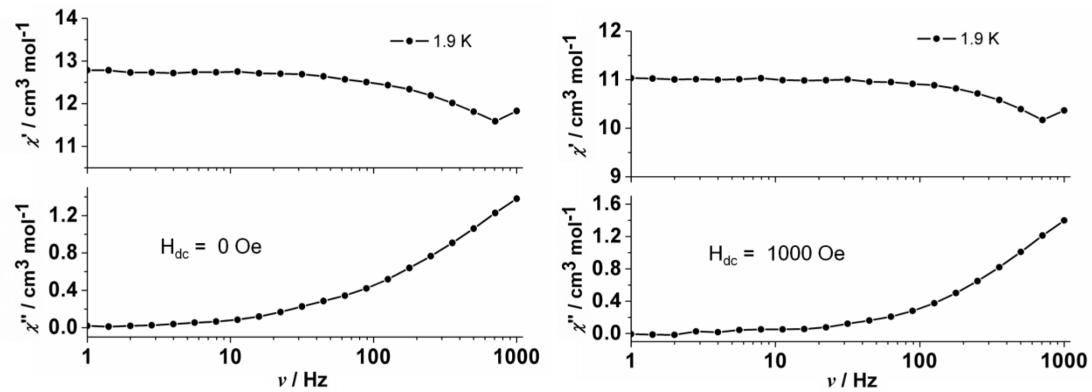

Fig. S7. Frequency-dependent in-phase χ' and out-of-phase χ'' ac susceptibility signals for **1** at the temperature of 1.9 K under zero and 1000 Oe dc field, respectively.

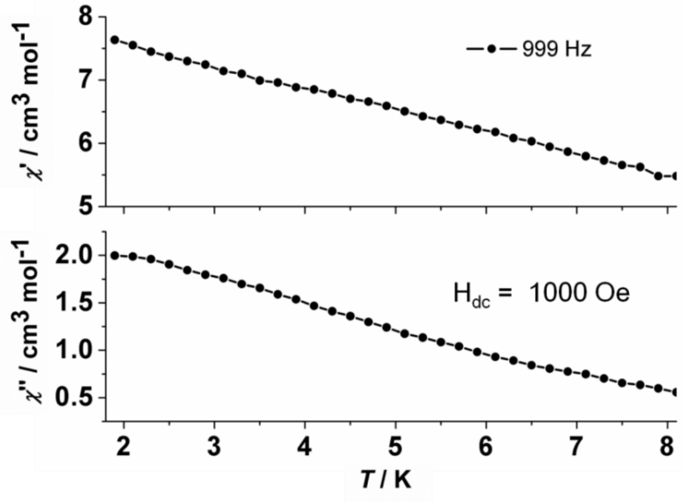

Fig. S8. Temperature-dependent in-phase χ' (right) and out-of-phase χ'' (left) ac susceptibility signals for **4** at the frequency of 999 Hz under 1000 Oe dc field.

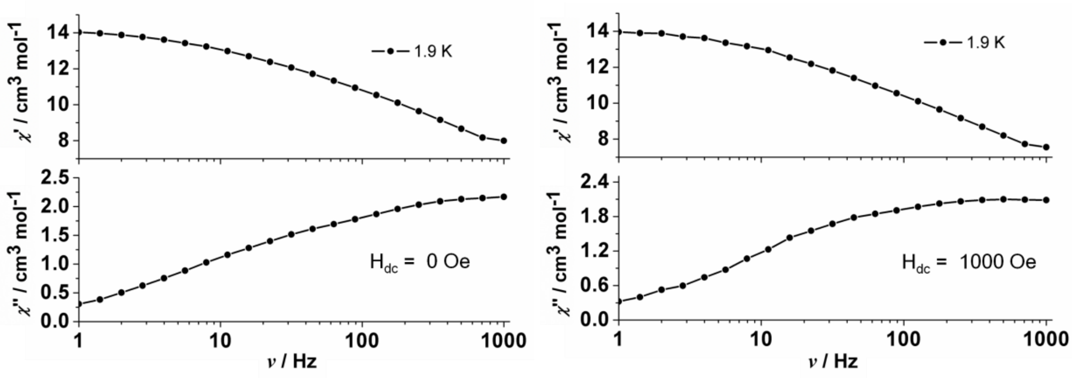

Fig. S9. Frequency-dependent in-phase χ' and out-of-phase χ'' ac susceptibility signals for **4** at the temperature of 1.9 K under zero and 1000 Oe dc field, respectively.

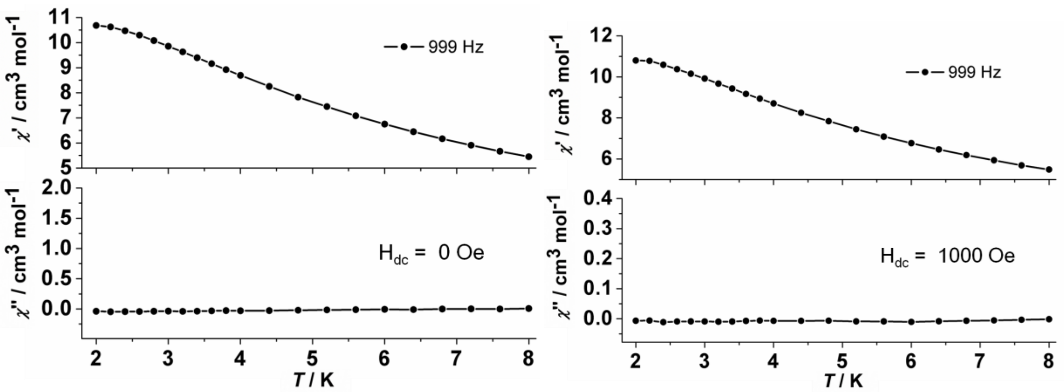

Fig. S10. Temperature-dependent in-phase χ' and out-of-phase χ'' ac susceptibility signals for **2** at the frequency of 999 Hz under zero and 1000 Oe dc field, respectively.

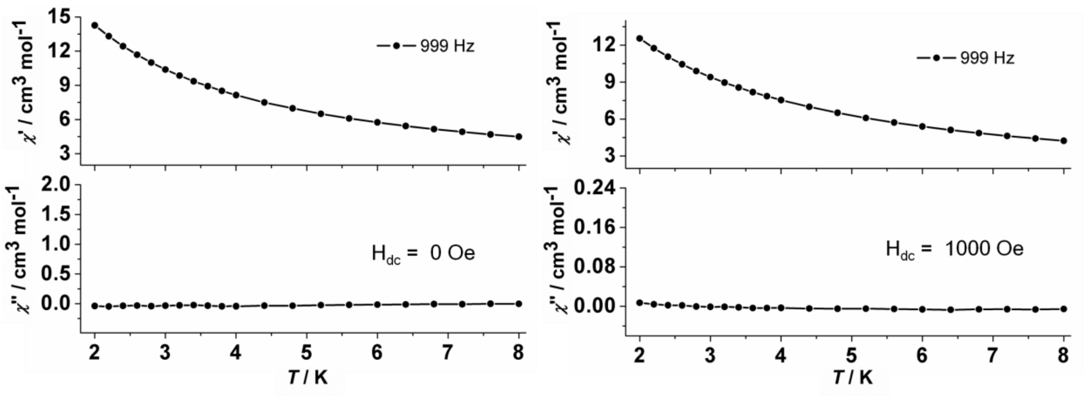

Fig. S11. Temperature-dependent in-phase χ' and out-of-phase χ'' ac susceptibility signals for **3** at the frequency of 999 Hz under zero and 1000 Oe dc field, respectively.

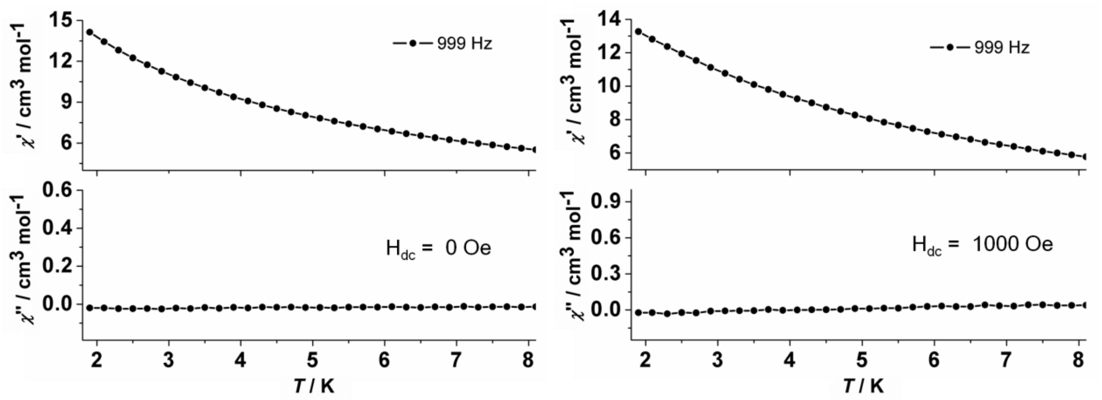

Fig. S12. Temperature-dependent in-phase χ' and out-of-phase χ'' ac susceptibility signals for **5** at the frequency of 999 Hz under zero and 1000 Oe dc field, respectively.

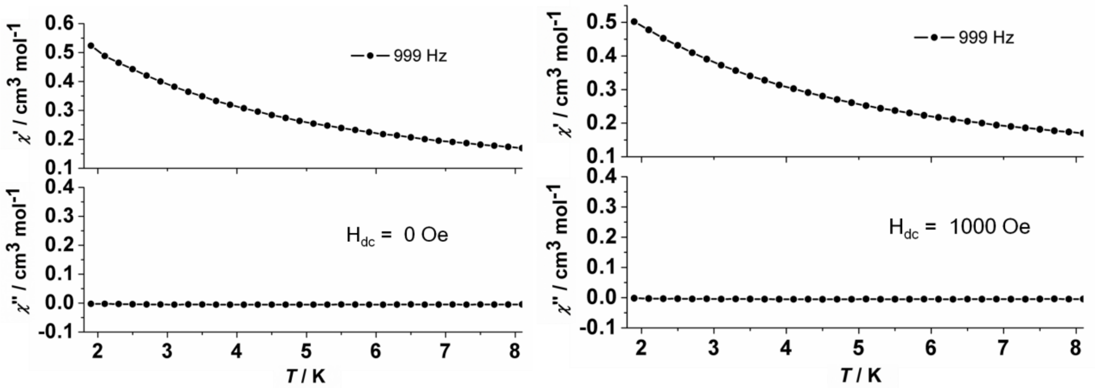

Fig. S13. Temperature-dependent in-phase χ' and out-of-phase χ'' ac susceptibility signals for **6** at the frequency of 999 Hz under zero and 1000 Oe dc field, respectively.